Absorption Spectra of Caffeic Acid, Caffeate and Their 1:1 Complex with Al(III): Density Functional Theory and Time-Dependent Density Functional Theory Investigations

Jean-Paul Cornard* and Christine Lapouge

LASIR, CNRS UMR 8516, Université des Sciences et Technologies de Lille,
Bât C5-59655 Villeneuve d'Ascq Cedex, France

The UV−visible absorption spectra of caffeic acid, caffeate and of the predominant complex obtained in the presence of aluminum ion (1:1 stoichiometry) have been simulated by using the time-dependent density functional theory (TD-DFT) technique, taking into account solvent effects. Whereas the use of the B3LYP hybrid XC functional with the 6-31+G(d,p) basis set allows us to reproduce fairly well the essential features of the experimental spectra of caffeic acid and caffeate, it is necessary to introduce an effective core potential to properly describe the aluminum ion and its environment and to obtain a good agreement between theoretical and experimental spectra of the 1:1 complex. The ligand presents two potential complexing sites in competition. The results of our calculations show that the aluminum ion coordinates preferentially at the level of the catecholate group, and the $[Al(H_2O)_4(CA)]$, $[Al(H_2O)_3(OH)(CA)]^-$ and $[Al(H_2O)_4(HCA)]^+$ complexed forms could coexist in aqueous solution at pH = 5.

1. Introduction

Acidic precipitation caused by human activity results in increased aluminum concentrations in natural waters and soil solutions.[1] Natural organic matter plays an important role in the speciation and geochemistry of aluminum in natural systems.[2] The $Al^{3+}-H^+$ exchange reactions on organic matter exchange sites are important sources of pH buffering in soils and control the Al(III) activity in acid soils.[3,4] The toxicity of Al(III) in natural environments is an important limiting factor for plant growth and root development in acidic soils.[5] The metal complexation by the organic matter changes the speciation of Al(III) and influence its toxicity. Organic matter in the environment can be divided into two classes of compounds: nonhumic material (e.g., protein, polysaccharides, nucleic acid) and humic substances.[6] These last substances are macromolecular systems that constitute the major fraction (60−70%) of soil organic matter. They consist of nonuniform distribution of functional groups joined by a variety of aliphatic and aromatic units. The carboxylic, phenolic and carbonyl functions are the most abundant and most influential in regard to metal complexation.[7] To gain a greater understanding of these complexation reactions and of their mechanisms, it is useful to apply spectroscopic techniques combined with quantum chemical calculations to model compounds containing functional groups that are present in the polymeric substances. Our works consist of the comparison of the chelating power of different types of binding site toward metal ions. The complexation mechanisms of Pb(II) and Al(III) with polyphenolic compounds such as flavonoids or cinnamic acid have been investigated to propose a classification of the different functional groups according to their ability to form chelates.[8−13]

Caffeic acid, *trans*-3-(3,4-dihydroxyphenyl)propenoic acid, constitutes a precursor compound in the formation of soil organic matter and participates in the transport of ionic metals present in the soil.[14] This ligand presents two complexing sites in competition: the catechol group (dihydroxybenzene) and the carboxylic function. In a recent work, we have shown that in water solution, at pH = 6.50, the lead(II) metal ion preferentially coordinates to the carboxylate function of caffeic acid, with the formation of a 1:1 complex for low amounts of lead(II).[15] This study has been carried out using molecular spectroscopies combined with quantum chemical calculations. Another study, concerning the Al(III)−caffeic acid system, showed that the first site involved in the complexation mechanism of Al(III) is the catechol group, and that the chelation occurs with a complete deprotonation of the two hydroxyl functions.[16] Nevertheless, this study was undertaken in methanol solution and no simple extrapolation can be made concerning the behavior of this ligand in aqueous solution. The purpose of this paper is to unambiguously determine which of the two potential chelating groups is preferentially involved in the binding of the aluminum(III) ion with caffeic acid, in aqueous solution at pH = 5.0, value close to the pH generally found in the soils.

The complexation mechanism of Al(III) by caffeic acid has been experimentally followed by UV−visible spectroscopy combined with chemometric methods. These techniques have allowed the determination of the stoichiometries and an estimation of the stability constants of the different complexes formed by successive addition of Al(III) in a caffeic acid solution in water by keeping a constant pH at 5.0.[17] From the spectral data set of the dosage, the electronic absorption spectrum of each pure species has been extracted. At pH = 5.0 and for low amounts of Al(III), the results of these experiments show that (i) the formation of a 1:1 complex is largely predominant, and (ii) the absorption spectrum of this complex fundamentally differs from that of the free ligand.

Time-dependent density functional theory (TD-DFT) has recently become a reliable method for calculation of excited-state energies and has proven its usefulness in the assignment of the electronic singlet excited states of the absorption spectra of systems as metal complex with organic molecules.[18−24] Molar

---

* Corresponding author. Tel: + 33-3.20.43.69.26. Fax: + 33-3.20.43.67.55. E-mail: cornard@univ-lille1.fr.

absorptivities were calculated on the basis of the values of oscillator strengths for the excited states and were found to be in close agreement with experimental ones. To determine the preferential complexing site of caffeic acid toward Al(III), we propose in this paper to calculate the electronic absorption spectra for all the possible structures of the complex and to compare them to the experimental features.

The first pK_a, corresponding to the deprotonation of the carboxylic function of caffeic acid, is close to 4.4.[17,25−28] So, at pH = 5.0 in water, the solution is a mixture of caffeic acid (26%) and caffeate (74%). In the same way, dissolved in water, aluminum occurs as many different species. The most toxic aqueous Al forms are Al^{3+} and Al hydroxy species ($Al(OH)^{2+}$, $Al(OH)_2{}^+$and $Al(OH)_4{}^-$),[29,30] the concentrations of the dominant species are shown to vary with pH, water temperature and ionic strength.[31,32] Thus all the possibilities of complexation between aluminum and caffeic acid in their various forms will have to be considered.

2. Experimental and Theoretical Methods

2.1. Reagents, Preparative Methods and Instrumentation. Caffeic acid was obtained commercially from Sigma. Al^{3+} stock solutions were prepared from aluminum chloride $AlCl_3 \cdot 6H_2O$. For all working solutions, sodium chloride has been added to give a constant ionic strength of 0.10 M. The molar ratio method has allowed the determination of the complexes composition in solution from UV−visible spectra. In this method, the electronic spectra of solutions containing a constant concentration of caffeic acid in water (5 × 10^{-5} M) and variable concentration of $AlCl_3$ were recorded. The titrations were effected by incremental additions of aluminum chloride and additions of NaOH to keep pH = 5. A Minipuls II (Gibson) peristaltic pump was used to circulate solution from the thermostated titration cell (25 °C) to the flow cell (Hellma) for absorption measurements. Due to the dilution of the ligand solution, all the electronic spectra were corrected before exploitation. UV−visible spectra were run on a double-beam spectrophotometer (Cary 100-Varian) using flow cells of 1 cm path length.

2.2. Chemometrics Methods. The UV−visible spectra were refined by using a multivariate data analysis program for modeling and fitting equilibrium titration 3D data sets (SPECFIT software, version 3.0.32).[33] The set of spectra obtained at variable Al(III) concentration were treated by evolving factor analysis (EFA)[34] to determine the number of different species in the system and the pure absorption spectrum of each species.

2.3. Quantum Chemical Calculations. All calculations were performed at the density functional level of theory with the hybrid functional B3LYP,[35,36] using the Gaussian (G03) program package.[37] Geometry optimizations were carried out, without any symmetry constraints, using the 6-31+G(d,p) basis set, including polarization functions to correctly take into account intramolecular H-bonding in the ligand. Diffuse functions have been added on the heavy atoms, to achieve a good description of anions. For sake of homogeneity, this basis set was employed for all species, whatever their charge. The double-ξ LANL2DZ pseudopotential has also been used for the description of the metal atom. Vibrational frequency calculations have been performed to ensure that all the optimized structures of free and complexed ligands correspond to energy minima. Bond orders have been computed with the Border Program (Version 1.0)[38,39] from the Gaussian molecular orbitals, and atomic charges were estimated in the NPA approach.[40] The low-lying excited states were treated within the adiabatic approximation
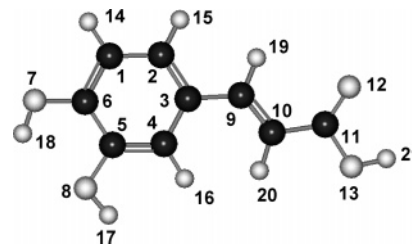
Figure 1. Most stable structure of caffeic acid and atomic numbering used in the text.

of time-dependent density functional theory (DFT-RPA)[41] with the B3LYP hybrid functional. Vertical excitation energies were computed for the first 40 singlet excited states, to reproduce the UV−visible spectra of free and complexed ligands. As it is well-known that the UV−visible absorption spectra are very sensitive to the solvent effects, these latter were introduced by the SCRF method, via the Polarized Continuum Model (IEF-PCM)[42] implemented in the Gaussian program.

3. Results and Discussion

3.1. Theoretical Absorption Spectra of Free Ligands. The molecular structure of caffeic acid (H_3CA) has already been studied using DFT methods (B3LYP/6-31G(d,p)).[15,16,43] We started our TD-DFT calculations from the most stable conformer of H_3CA, which presents a planar structure, with an intramolecular hydrogen bond at the catechol level. With regard to caffeate (H_2CA^-), no structural information was reported in the literature, and the most stable conformation of this ion was calculated at the B3LYP/6-31+G(d,p) level of theory. To make a comparison of the structures of H_3CA and H_2CA^-, and to observe the structural modifications caused by the deprotonation of the acid function, the geometry of H_3CA was also optimized with the 6-31+G(d,p) basis set. As one could expect, the structural parameters of the neutral molecule are very little affected by taking into account the diffuse functions in the 6-31+G(d,p) basis set, differences of only 0.002 Å are observed for the bond lengths. The atom numbering of H_3CA used in this paper is reported in Figure 1. The calculated bond lengths of both caffeic acid and caffeate are given in the two first columns of Table 1. Complete geometric details of these systems are provided as Supporting Information (Tables S1). The deprotonation of the carboxylic group does not cause substantial changes in the bond lengths and angles of the benzene ring. It is obvious that $C_{11}O_{12}$ and $C_{11}O_{13}$ bonds are particularly affected by the deprotonation. An increase of the $C_{11}O_{12}$ bond length, accompanied by a shortening of the $C_{11}O_{13}$ bond, is observed for the caffeate, where these two bonds become equivalent. The length of the adjacent bond $C_{10}C_{11}$ increases of 0.073 Å, and in a general way, the electronic delocalization along the carbon chain tends to slightly decrease in H_2CA^-. The deprotonation has a low effect on the hydroxyl functions of the catechol group. The C−O bond length increases in caffeate, notably the C_6O_7 bond which is longer by 0.033 Å compared to H_3CA. In the same way, the O_8- - -H_{18} intramolecular hydrogen bond is slightly stronger in the ion than in the neutral molecule.

To better evaluate the structural and electronic changes accompanying deprotonation, we have completed these data by a calculation of the bond orders and atomic charges (NPA) for both neutral and anionic compounds. At the 6-31+G(d,p) level of theory, appreciably too high bond orders between nonbonding atoms are computed, which is probably due to a too strong overlap of diffuse atomic orbitals on the heavy atoms. When diffuse functions are omitted, with the 6-31G(d,p) basis set, the

Absorption Spectra of Caffeic Acid and Caffeate

J. Phys. Chem. A, Vol. 110, No. 22, 2006 **7161**

TABLE 1: Bond Lengths (Å) and Bond Orders Calculated for Protonated and Deprotonated Caffeic Acid

	bond lengths 6-31+G(d,p)		bond orders 6-31G(d,p)	
	caffeic acid	caffeate	caffeic acid	caffeate
C1C2	1.394	1.396	1.42	1.41
C2C3	1.407	1.408	1.37	1.39
C3C4	1.413	1.412	1.33	1.35
C4C5	1.384	1.385	1.43	1.42
C5C6	1.410	1.404	1.27	1.29
C6C1	1.393	1.391	1.42	1.43
C3C9	1.458	1.466	1.11	1.07
C9C10	1.350	1.343	1.69	1.76
C10C11	1.470	1.543	1.05	0.94
C6O7	1.359	1.392	0.98	0.95
C5O8	1.378	1.388	0.92	0.90
C11O12	1.220	1.257	1.79	1.63
C11O13	1.364	1.258	1.49	1.58
C1H14	1.085	1.086	0.93	0.93
C2H15	1.086	1.086	0.94	0.94
C4H16	1.087	1.088	0.92	0.92
O8H17	0.966	0.965	0.83	0.84
O7H18	0.970	0.969	0.83	0.83
C9H19	1.089	1.090	0.93	0.92
C10H20	1.085	1.092	0.93	
O13H21	0.972		0.83	
O8---H18	2.147	2.118		

TABLE 2: NPA Charges of Caffeic Acid and Caffeate Ion Calculated at the B3LYP/6-31+G(d,p) Level of Theory

	caffeic acid	caffeate
C1	−0.28	−0.28
C2	−0.20	−0.24
C3	−0.11	−0.06
C4	−0.27	−0.29
C5	0.25	0.24
C6	0.30	0.25
C9	−0.13	−0.28
C10	−0.36	−0.26
C11	0.77	0.73
O7	−0.70	−0.73
O8	−0.74	−0.76
O12	−0.62	−0.78
O13	−0.73	−0.77
H14	0.26	0.24
H15	0.24	0.25
H16	0.24	0.24
H17	0.52	0.52
H18	0.53	0.52
H19	0.26	0.26
H20	0.24	0.20
H21	0.52	

Figure 2. UV−visible spectrum recorded in aqueous solution and positions of the electronic transitions calculated in water of (a) caffeic acid and (b) caffeate. The height of the vertical lines is proportional to the calculated oscillator strength.

results seem consistent and are reported in Table 1. The variations observed in the bond orders between the neutral and anionic forms confirm that the main modifications take place at the level of the acid function and the carbonaceous chain. The C_9C_{10} bond adopts a more pronounced double character in H_2CA^- than in H_3CA, whereas the C_3C_9 and $C_{10}C_{11}$ bonds have a single bond character in the ion. The atomic charges obtained through the NPA methods are shown in Table 2. Except for the C_3 and C_{10} atoms, the charge of all the atoms become more negative in H_2CA^-, showing a complete delocalization of the negative charge overall the caffeate ion. The charges that undergo the greatest alterations were those of the carbon chain atoms, notably the C_9 and C_{10} atoms, and the O_{12} oxygen atom.

All the observations suggest that the electronic delocalization between the benzene ring and the carboxylic or carboxylate function is relatively low in H_3CA and still decreases with the deprotonation of the acid function.

The experimental and calculated (vertical lines) electronic

absorption spectra of H_3CA and H_2CA^- are presented in Figure 2. The experimental UV−vis spectra (a) and (b) have been recorded from an aqueous solution of caffeic acid at pH = 2 and 6.5, respectively, where only one species is present in solution. Inclusion of solvation effects introduces relevant changes to the theoretical spectrum with respect to that computed in vacuo, in terms of both absorption wavelengths and oscillator strengths. For reasons of clearness, only the results obtained by taking into account the solvent effects are reported. The theoretical spectrum of H_3CA is in fairly good agreement with the experimental one both in wavelengths and in intensity. All the experimental features can be depicted by a computed electronic transition. The deprotonation of the acid function completely modifies the shape of the absorption spectrum. The hypsochromic shift observed for the absorption band lying in the long wavelengths range is well reproduced by the calculations. However, the agreement between the theoretical and experimental spectra of the anion is slightly less good than that obtained for the neutral molecule. Indeed, the second transition in the long wavelengths is calculated 12 nm too low compared to the experimental one. Nevertheless, one can note that the low energy transition is estimated with the same accuracy as for the neutral form. Table 3 lists the molecular orbitals involved in the calculated transitions, only the contributions higher than 10% were reported. Except for the transition of weaker energy, which mainly implies the HOMO and LUMO orbitals, the other computed transitions present very different origins in the spectra of H_3CA and H_2CA^-, respectively.

The main MO's involved in the electronic transitions calculated for the neutral and ionic forms are depicted in Figure 3. The shapes of the orbitals of H_3CA calculated in water are the same as those calculated in methanol solution.[16] All the electronic transitions observed in the absorption spectrum of the neutral molecule have a $\pi\pi^*$ character. In opposition, among its frontier orbitals, the anion presents MO's with totally

**TABLE 3: Experimental and Calculated (B3LYP/
6-31+G(d,p)) Absorption Wavelengths of Caffeic Acid and
Caffeate**[a]

caffeic acid				caffeate			
λ_{exptl} (nm)	λ_{calc} (nm)	f	MO contribution (%)	λ_{exptl} (nm)	λ_{calc} (nm)	f	MO contribution (%)
321	326	0.57	H → L (78)	309	303	0.56	H → L (78)
292	288	0.19	H−1 → L (81)	283	271	0.15	H−2 → L (61)
							H → L+1 (28)
235	239	0.09	H → L+1 (68)	240	241	0.14	H → L+1 (43)
			H−3 → L (11)				H−2 → L (22)
							H−4 → L (16)
216	217	0.12	H−3 → L (70)	213	214	0.13	H−5 → L (55)
							H → L+5 (34)
sh	204	0.10	H → L+2 (54),	213	210	0.36	H−2 → L+1 (50)
			H−1 → L+1 (34)				H → L+5 (26)
							H−5 → L (11)
				sh	203	0.05	H−1 → L+3 (55)
							H−1 → L+2 (27)

[a] Only the transitions with high oscillator strengths f and molecular
orbital contributions >10% are reported. sh: shoulder.
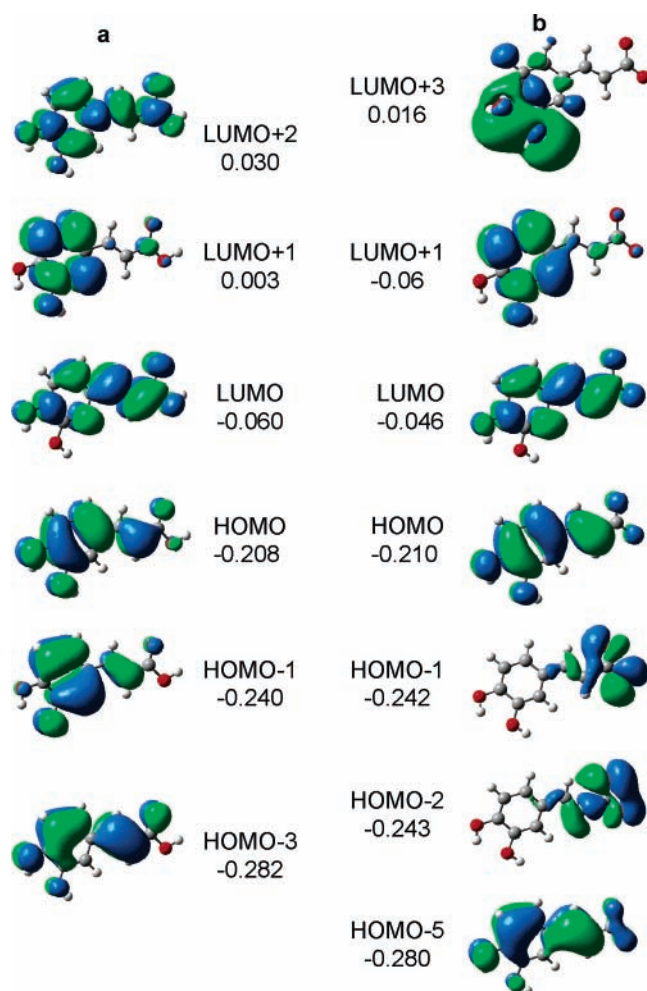
Figure 3. Molecular frontier orbitals involved in the main calculated
vertical transitions of (a) caffeic acid and (b) caffeate ion. The energy
of the MO is in electronvolts.

different character. Thus, the HOMO−1 and HOMO−2, which
have roughly the same energy, are nonbonding orbitals localized
on the carbonyl group; they are obtained respectively by out-
of-phase and in-phase combinations of p atomic orbitals on the
O atoms, in the molecular plane. In the same way, the LUMO+3
is localized on the O−H bonds of the catechol group and has
a σ^* character. Whereas the HOMO, LUMO and LUMO+1 of

H_2CA^- have shapes very similar to those calculated for H_3CA,
they differ in energy.

The first absorption band located in the long wavelengths of
the H_2CA^- spectrum has the same origin as that observed for
H_3CA and corresponds to a transition principally involving the
HOMO−LUMO (78%); the blue shift of this band noticed upon
deprotonation results from a different HOMO−LUMO gap
(0.148 and 0.164 eV for H_3CA and H_2CA^-, respectively). The
assignment of the other bands of the two spectra differs totally
and explains the pronounced changes of the spectral features.
The band calculated at 271 nm for H_2CA^- corresponds to a
mixture of n → π^* and π → π^* transitions; it consists of a
charge transfer from the carboxylate and the carbonaceous chain
toward the benzene ring. In a same manner, the transitions
calculated at 241 and 210 nm mix n → π^* and π → π^*
characters (L+5 presenting a π^* character). The transition
computed at 203 nm, with a very low value of the oscillator
strength (0.05) puts together n → σ^* and n → π^* characters
(L+2 presenting a π^* character).

3.2. Theoretical Absorption Spectra of Complexes. Our
previous study[17] has shown that, in aqueous solution at pH =
5, caffeic acid leads to the simultaneous formation of several
complexes in the presence of Al(III). For low amounts of $AlCl_3$
added to the solution, the chemometric methods allow the
determination of two spectra of pure species corresponding to
complexes of 1:1 and 1:2 stoichiometry (metal:ligand). The
concentration curves of the complexed forms versus the quantity
of aluminum added show that the 1:1 complex is very largely
predominant compared to the 1:2 complex. In these two species,
it is easily conceivable that only one site of complexation is
involved. For [Al(III)]/[ligand] molar ratios higher than 0.1, the
formation of a new species of 2:1 stoichiometry is observed. In
this binuclear complex, two aluminum ions are simultaneously
coordinated to the two complexing sites of the ligand. The fact
that the second complexation site is implied in the metal
coordination whereas less than 10% of the first sites are occupied
indicates that the catechol and the carboxylic or carboxylate
functions present nearby capacities of complexation for this
molecule, under the used physicochemical conditions.

As in the natural environments, the polluting metal concentra-
tion is weak compared to the number of potential binding sites,
we were interested only in the first complex formed in a
predominant way: the 1:1 complex. The chemometric methods
made it possible to determine only one UV−visible absorption
spectrum corresponding to the 1:1 complex. This spectrum is
either the spectrum of a pure species or the algebraic sum of
the absorption of various species of 1:1 stoichiometry, which
would present very close spectra impossible to distinguish. At
25 °C and pH = 5, the calculated distribution of dissolved
inorganic aluminum ions in water shows that the predominant
species are Al^{3+} and $Al(OH)^{2+}$; $Al(OH)_2^+$ is in minor concen-
tration, whereas the concentration of $Al(OH)_3$ is totally negli-
gible.[44] From the two forms of the ligand (H_3CA and H_2CA^-)
and prevalent forms of Al(III) in solution (Al^{3+} and $Al(OH)^{2+}$),
we considered the various possible combinations of associations
by considering a complexation either at the level of the catechol
function or on the acid group. Starting from the optimized
molecular structure, the electronic absorption spectrum was
calculated for each possible combination, by taking into account
the solvent effects. In all cases, we considered an octahedral
environment for the aluminum atom and, consequently, added
water molecules to supplement the valence of this one. It should
also be noted that the complexation at the level of the catechol
function gives a bidentate complex and that the formation of

Absorption Spectra of Caffeic Acid and Caffeate

J. Phys. Chem. A, Vol. 110, No. 22, 2006 **7163**
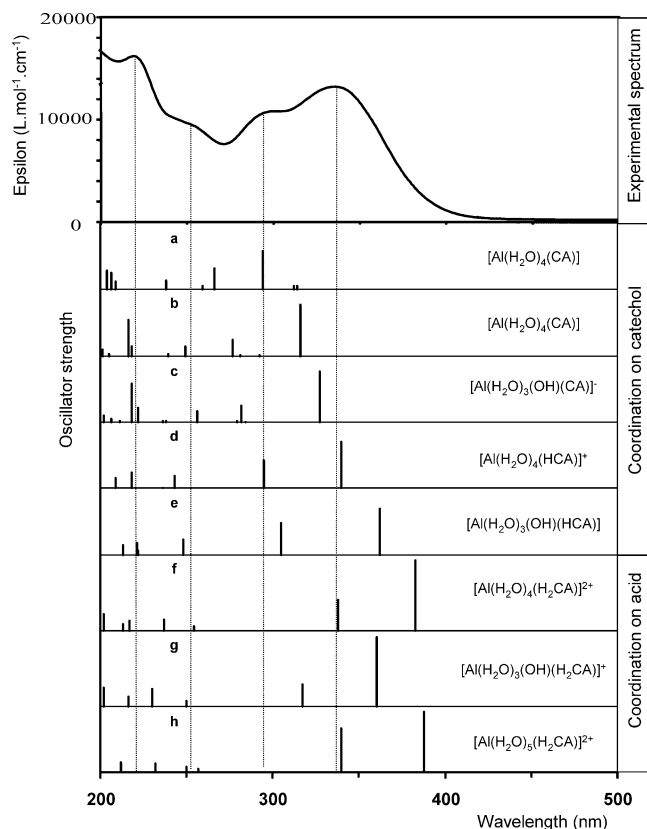
Figure 4. Experimental electronic spectrum of 1:1 complex (obtained by chemometric methods) and theoretical absorption spectra calculated for different species: (a) B3LYP/6-31+G(d,p); (b)−(h) B3LYP/6-31+G(d,p)/LANL2DZ.

this chelate is accompanied by a double deprotonation of the hydroxyl groups.[10,16,45−47]

Experimentally, the addition of AlCl₃ to a caffeic acid solution at pH = 5 leads to a bathochromic shift of the absorption band in the long wavelengths. The UV−visible spectrum of the 1:1 complex extracted from the experimental data set using chemometric methods is presented in the Figure 4. This spectrum shows broad bands with maxima located at 335, 292, 250 and 218 nm.

In a first step, we have considered a complexation with the dianionic catecholate species in a chelating configuration with a (i) deprotonated and (ii) protonated acid group. The results of the geometry optimization of the [Al(H₂O)₄(CA)] complex with the 6-31+G(d,p) basis set show that if the ligand remains planar, the aluminum atom is out of this plane, with a computed dihedral angle value of 15°. The theoretical spectrum (Figure 4a) corresponding to [Al(H₂O)₄(CA)] presents a poor agreement

with the experimental one both in wavelengths and in intensity. The transition involving predominantly the HOMO−LUMO is calculated at 293 nm. Two other transitions calculated with higher wavelengths (314 and 312 nm) present very low oscillator strength values and mainly involve HOMO−1 → LUMO and HOMO−2 → LUMO, respectively. The main problem lies in the fact that the LUMO has a σ* character and is exclusively localized on the water molecules. Consequently all the absorption bands calculated in the long wavelengths range result from n → σ* or π → σ* transitions, what appears to be a unreliable spectral attribution for such a chemical system. This result means that the aluminum atom and its environment in the considered complex are very badly described by the calculation method using the 6-31+G(d,p) basis set. Other basis sets, such as the 6-311G(d, p), were tested and did not give any improvement to the results. For this reason, other calculations were carried out by using the LANL2DZ pseudopotential to describe the aluminum atom and the 6-31+G(d,p) basis set for the remainder of the compound. For the complex geometry optimization, the introduction of a pseudopotential in the calculations gives results appreciably different from those obtained previously, with in particular, the aluminum atom localized in the ligand plane. The theoretical spectrum (Figure 4b) calculated with 6-31+G(d,p)/LANL2DZ is more in agreement with the experimental features than spectrum a. But the most important point is that the HOMO → LUMO transition, calculated at 316 nm and corresponding to the strong optical absorption observed at 335 nm, presents a ππ* character, as expected for such system. The use of a pseudopotential to describe the Al atom leads to a reliable assignment of electronic transitions and makes us think that a better description of the studied chemical system is then obtained. In a similar way, the absorption bands recorded in the low wavelengths range are also well described by theoretical transitions. Consequently, it is possible to affirm that the [Al-(H₂O)₄(CA)] complexed form can take part to a certain extent in the shape of the experimental spectrum of the 1:1 complex. This observation is much more justified for the [Al(H₂O)₃(OH)-(CA)]⁻ complexed form of which the theoretical spectrum (Figure 4c) is even closer to the experimental one, both in wavelengths and in intensity on all the spectral range. The HOMO → LUMO transition calculated at 327 nm and the HOMO−1 → LUMO transition calculated at 282 nm are relatively close to the experimental values. In a similar way, the bands located at 250 and 218 nm in the UV−visible spectrum can be easily assigned to the transitions computed at 256 and 218 nm, respectively. Moreover, the oscillator strengths of all the calculated transitions are proportional to the absorbance measured on the spectrum. If one now considers the ligand protonated at the level of the acid function with a Al(III)

TABLE 4: Computed Wavelengths (B3LYP/6-31+G(d,p)/LANL2DZ) and Oscillator Strengths (*f*) for the Optical Transitions with *f* > 0.10 of the Different Complexed Forms, in Terms of Single Molecular Orbital Excitations with Percentages Larger Than 10%

	[Al(H₂O)₄(CA)]			[Al(H₂O)₃(OH)(CA)]⁻			[Al(H₂O)₄(HCA)]⁺		
λ_{exptl} (nm)	λ_{calc} (nm)	*f*	MO contribution (%)	λ_{calc} (nm)	*f*	MO contribution (%)	λ_{calc} (nm)	*f*	MO contribution (%)
335	316	0.55	H → L (80)	327	0.53	H → L (81)	340	0.49	H → L (79)
292	277	0.17	H−1 → L (59) H → L+2 (19)	282	0.18	H−1 → L (65) H → L+2 (20)	294	0.29	H−1 → L (82)
250	249	0.11	H → L+2 (60) H−1 → L (19)	255	0.11	H → L+2 (61) H−1 → L (19)	243	0.14	H → L+1 (71) H−3 → L (10)
218	216	0.38	H−5 → L (37) H−1 → L+2 (34)	222	0.15	H−1 → L+7 (46) H−1 → L+2 (31)	218	0.17	H−3 → L (73)
				218	0.41	H−5 → L (50) H−1 → L+2 (26)	209	0.11	H → L+3 (61) H−1 → L+1 (29)
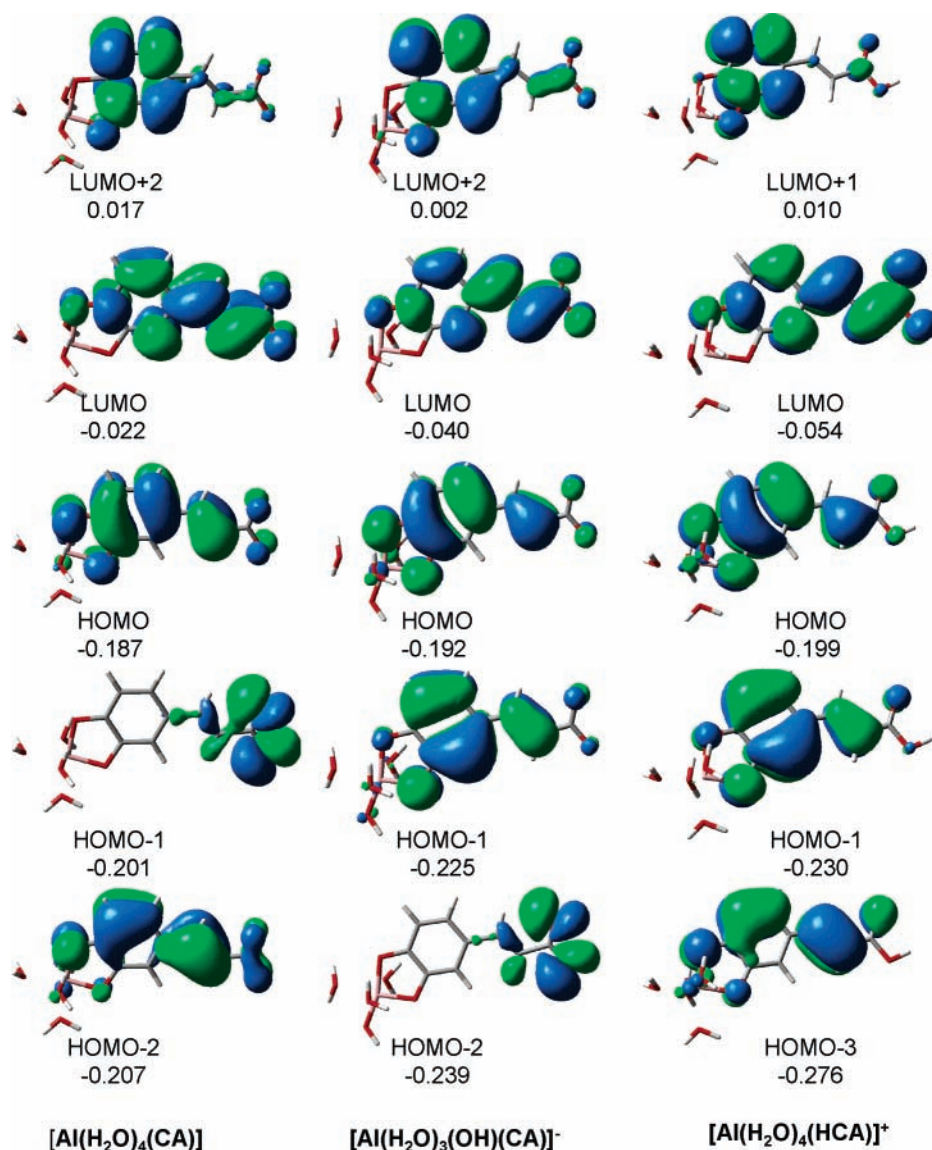
Figure 5. Main molecular frontier orbitals involved in the calculated electronic transitions of the three possible complexed forms present in solution at pH = 5. The energy of the MO is in electronvolts.

chelation on the catechol, it can be observed that the complex $[Al(H_2O)_4(HCA)]^+$ (Figure 4d) has a theoretical spectrum extremely close to that recorded, whereas the complex $[Al(H_2O)_3(OH)(HCA)]$ (Figure 4e) presents much more marked differences. Indeed, the HOMO−LUMO transition is calculated 28 nm too high and the intensities in the short wavelengths range are not fairly reproduced. To summarize, with regard to a possible chelation via the catechol group, one observes with the experimental spectrum a very good agreement for the theoretical spectrum of $[Al(H_2O)_4(HCA)]^+$ and an average agreement for the species $[Al(H_2O)_3(OH)(CA)]^-$ and $[Al(H_2O)_4(CA)]$, and consequently these three species must have a nonnegligible contribution in the optical absorption of the complex 1:1.

In a second step, Al(III) complexation through the carboxylate function has been envisaged. The theoretical spectra (Figure 4f,g) of the two chelates $[Al(H_2O)_4(H_2CA)]^{2+}$ and $[Al(H_2O)_3(OH)(H_2CA)]^+$, respectively, present a very bad agreement with the experimental spectrum of the 1:1 complex. In particular, the two transitions of weaker energy are completely shifted toward the long wavelengths compared with the observed absorption bands (+47 and +26 nm for the HOMO−LUMO transitions, respectively). It is the same if a monodentate

complex $[Al(H_2O)_5(H_2CA)]^{2+}$ is considered (spectrum h). Its theoretical spectrum is close to that of the $[Al(H_2O)_4(H_2CA)]^{2+}$ species, with a HOMO−LUMO transition calculated at 388 nm. Thus, it would seem that the possibility of a coordination of Al(III) on the carboxylate site could be ruled out for the 1:1 complex.

All the results, illustrated by Figure 4, show that the coordination of Al(III) takes place at the catecholate function, whatever the protonation state of the carboxylic group, in low acidic aqueous medium. Thus, the behavior of Al(III) with this ligand in water at pH = 5 is the same as that observed in methanol solution[16] with, however, a possible deprotonation of the carboxyl. In the remainder of this paper, we reported the spectral assignments of only the $[Al(H_2O)_4(CA)]$, $[Al(H_2O)_3(OH)(CA)]^-$ and $[Al(H_2O)_4(HCA)]^+$ complexed forms for which the theoretical spectra are closest to the experimental spectrum. Table 4 presents the molecular orbitals involved in the calculated transitions in the studied spectral range. For the three compounds, the transition in the long wavelengths mainly consists of the HOMO → LUMO, with an average contribution of 80%. These frontier orbitals have similar shapes for all the complexes, whatever the charge of this one and whatever the protonation state of the carboxylic function but differ slightly in energy

Absorption Spectra of Caffeic Acid and Caffeate

J. Phys. Chem. A, Vol. 110, No. 22, 2006 **7165**

(Figure 5); these MO are very close to those of the free ligands (caffeic acid and caffeate). The nature of the HOMO → LUMO transition is essentially of the $\pi\pi^*$ type and is calculated in all cases with a high value of the oscillator strength. In opposition, the assignment of the absorption band observed at 292 nm differs according to the complex. In the three cases, if the HOMO−1 → LUMO transition is preponderant, the nature of the HOMO−1 is not the same for all the compounds. For [Al-$(H_2O)_4(CA)$], a n → π^* transition is found, whereas for $[Al(H_2O)_3(OH)(CA)]^-$ and $[Al(H_2O)_4(HCA)]^+$ the $\pi \to \pi^*$ character is largely predominant. In fact, an inversion in energy is observed for the HOMO−1 and HOMO−2 orbitals in the two complexes obtained starting from the caffeate ([Al(H_2O)_4-(CA)] and $[Al(H_2O)_3(OH)(CA)]^-$). In the same way, notable differences are observed for the three compounds in the assignment of the electronic absorption bands located in the short wavelengths range.

4. Conclusion

The results of this study provide further information regarding the complexation of Al(III) ion with caffeic acid, which can be considered as a model molecule of humic substances, insofar as this molecule presents two complexation sites in competition, which are very largely observed in the organic matter of the soils. At pH = 5 in aqueous solution, the addition of low amounts of Al(III) to caffeic acid leads to the formation of a predominant species of 1:1 stoichiometry. The results of our calculations, using the TD-DFT approach, have shown that the theoretical absorption spectra corresponding to a coordination of Al atom on the catecholate function are in good agreement with the experimental spectrum. On the other hand, a coordination of the metal ion with the acid function can be rejected at the sight of the poor agreement between theoretical and experimental UV−visible spectra. Under such physicochemical conditions, the catechol site thus presents a complexing capacity with respect to aluminum higher than that of the acid function. It should be noted that, on the contrary, the Pb(II) ion preferentially coordinates to the carboxylic function of caffeic acid.

For such a study, the use of the electronic spectroscopy has the great advantage of being able to work with very weak metal concentrations, which is the case in the natural environments. But generally, this spectroscopic technique compared to others presents the disadvantage of providing only little information of structural nature on the studied chemical system. Thus, this work shows that the contribution of the TD-DFT methodology allows us, from the UV−visible spectrum of a multisite ligand, to determine unambiguously the site preferentially involved in the coordination of a metal ion.

One can note that an energetic study could be interesting to explain these results and to validate the preferential chelating site of Al(III). However, a simple comparison of the energies of the different complexed forms is not reliable to determine the most stable one. Indeed, the complexation process involves numerous steps, as mono- or bi-deprotonations, and only reaction pathway calculations can provide valuable information.

Supporting Information Available: Table of angles and dihedral angles for caffeic acid and the caffeate ion. This material is available free of charge via the Internet at http://pubs.acs.org.

References and Notes

(1) Liu, T. W.; Huang, S. D. *Anal. Chem.* **2001**, *73*, 4319.
(2) Sposito, G. *The Environmental Chemistry of Al*; CRC Press: Boca Raton, FL, 1989.
(3) Bloom, P. R. *Soil Sci. Soc. Am. J.* **1979**, *43*, 815.
(4) Bloom, P. R. *Soil Sci. Soc. Am. J.* **1981**, *45*, 267.
(5) Wild, A. *Soils and the Environment: An Introduction*; Cambridge University Press: Cambridge, U.K., 1993.
(6) Stevenson, F. J. *Humus Chemistry: Genesis, Composition, Reactions*; Wiley: New York, 1982.
(7) Tiping, E. *Cation Binding by Humic Substances,* 1st ed; Cambridge University Press: Cambridge, U.K., 2002.
(8) Cornard, J. P.; Merlin, J. C. *Polyhedron* **2002**, *21*, 2801.
(9) Cornard, J. P.; Merlin, J. C. *J. Inorg. Biochem.* **2002**, *92*, 19.
(10) Cornard, J. P.; Merlin, J. C. *J. Mol. Struct.* **2003**, *651−653*, 381.
(11) Dangleterre, L.; Cornard, J. P. *Polyhedron* **2005**, *24*, 1593.
(12) Lapouge, C.; Cornard, J. P. *J. Phys. Chem. A* **2005**, *109*, 6752.
(13) Cornard, J. P.; Dangleterre, L.; Lapouge, C. *J. Phys. Chem. A* **2005**, *109*, 10044.
(14) Olsen, R. A.; Brown, J. C.; Bennett, J. H.; Blume, D. J. *J. Plant. Nutr.* **1982**, *5*, 433.
(15) Boilet, L.; Cornard, J. P.; Lapouge, C. *J. Phys. Chem. A* **2005**, *109*, 1952.
(16) Cornard, J. P.; Lapouge, C. *J. Phys. Chem. A* **2004**, *108*, 4470.
(17) Cornard, J. P.; Merlin, J. C. *Polyhedron*, in press.
(18) Fantacci, S.; De Angelis, F.; Selloni, A. *J. Am. Chem. Soc.* **2003**,*125*, 4381.
(19) Barone, V.; Fabrizi De Biani, F.; Ruiz, E.; Sieklucka, B. *J. Am. Chem. Soc.* **2001**, *123*, 10742.
(20) Gutierrez, F.; Rabbe, C.; Poteau, R.; Daudey, J. P. *J. Phys. Chem. A* **2005**, *109*, 4325.
(21) Han, Y. K.; Lee, S. U. *Chem. Phys. Lett.* **2002**, *366*, 9.
(22) Gao, H. Z.; Su, Z. M.; Qin, C. S.; Mo, R. G.; Kan, Y. E. *Int. J. Quantum Chem.* **2004,** *97*, 992.
(23) Zhang, J.; Frenking, G. *J. Phys. Chem. A* **2004**, *108*, 10296.
(24) Amati, M.; Lelj, F. *Chem. Phys. Lett.* **2002**, *358*, 144.
(25) Adams, M. L.; O'Sullivan, B.; Downard, A.; Powell, K. J. *J. Chem. Eng. Data* **2002**, *47*, 289.
(26) Kiss, T.; Navy, G. ; Pécsi, M. *Polyhedron* **1989**, *8*, 2345.
(27) Linder, P. W. ; Voyé, A. *Polyhedron* **1987**, *6*, 53.
(28) Lamy, I.; Seywert, M.; Cromer, M.; Scharff, J. P. *Anal. Chim. Acta* **1985**, *176*, 201.
(29) Gensemer, R. W.; Playle, R. C. *Crit. Rev. Environ. Sci. Technol.* **1999**, *29*, 315.
(30) Howells, G.; Dalziel, T. R. K.; Reader, J. P.; Solbe, J. F. In *Water Quality for Freshwater Fish*; Howells, G., Ed.; Gordon and Breach: London, 1994.
(31) Exley, C. *J. Inorg. Biochem.* **2003**, *97*, 1.
(32) Lydersen, E. *Nordic Hydrology.* **1990**, *21*, 195.
(33) Specfit Global Analysis System, Spectrum software Associates, Marlborough, MA.
(34) Gampp, H.; Maeder, M.; Meyer, C. J.; Zuberbühler, A. *Talanta* **1986**, *33*, 943.
(35) Becke, A. D. *J. Chem. Phys.* **1993**, *98*, 5648.
(36) Lee, C.; Yang, W.; Parr, R. G. *Phys. Rev. B* **1988**, *37*, 785.
(37) Frisch, M. J.; Trucks, G. W.; Schlegel, H. B.; Scuseria, G. E.; Robb, M. A.; Cheeseman, J. R.; Montgomery, J. A., Jr.; Vreven, T.; Kudin, K. N.; Burant, J. C.; Millam, J. M.; Iyengar, S. S.; Tomasi, J.; Barone, V.; Mennucci, B.; Cossi, M.; Scalmani, G.; Rega, N.; Petersson, G. A.; Nakatsuji, H.; Hada, M.; Ehara, M.; Toyota, K.; Fukuda, R.; Hasegawa, J.; Ishida, M.; Nakajima, T.; Honda, Y.; Kitao, O.; Nakai, H.; Klene, M.; Li, X.; Knox, J. E.; Hratchian, H. P.; Cross, J. B.; Adamo, C.; Jaramillo, J.; Gomperts, R.; Stratmann, R. E.; Yazyev, O.; Austin, A. J.; Cammi, R.; Pomelli, C.; Ochterski, J. W.; Ayala, P. Y.; Morokuma, K.; Voth, G. A.; Salvador, P.; Dannenberg, J. J.; Zakrzewski, V. G.; Dapprich, S.; Daniels, A. D.; Strain, M. C.; Farkas, O.; Malick, D. K.; Rabuck, A. D.; Raghavachari, K.; Foresman, J. B.; Ortiz, J. V.; Cui, Q.; Baboul, A. G.; Clifford, S.; Cioslowski, J.; Stefanov, B. B.; Liu, G.; Liashenko, A.; Piskorz, P.; Komaromi, I.; Martin, R. L.; Fox, D. J.; Keith, T.; Al-Laham, M. A.; Peng, C. Y.; Nanayakkara, A.; Challacombe, M.; Gill, P. M. W.; Johnson, B.; Chen, W.; Wong, M. W.; Gonzalez, C.; Pople, J. A. *Gaussian 03*, revision B.04; Gaussian, Inc.: Pittsburgh, PA, 2003.
(38) Mayer, I. Program "Border", version 1.0, Chemical Research Center, Hungarian Academy of Sciences, Budapest, 2005.
(39) Mayer, I. *Chem. Phys. Lett.* **1983**, *97*, 270.
(40) Reed, A. E.; Curtiss, L. A.; Weinhold, F. *Chem. Rev.* **1988**, *88*, 899.
(41) Bauernschmitt, R.; Ahlrichs, R. *Chem. Phys.* **1996**, *256*, 454.

(42) Cossi, M.; Scalmani, G.; Rega, N.; Barone, V. *J. Chem. Phys.* **2003**, *117*, 43.

(43) VanBesien, E.; Marques, M. P. M. *THEOCHEM* **2003**, *625*, 265.

(44) Lydersen, E. *Nordic Hydrology* **1990**, *21*, 195.

(45) Türkel, N.; Berker, M.; Özer, U. *Chem. Pharm. Bull.* **2004**, *52*, 929.

(46) Araujo, P. Z.; Morando, P. J.; Blesa, M. A. *Langmuir* **2005**, *21,* 3470.

(47) Lana-Villarreal, T.; Rodes, A.; Pérez, J. M.; Gomez, R. *J. Am. Chem. Soc.* **2005**, *127*, 12601.